International Journal of Environmental Sciences
ISSN: 2229-7359
Vol. 11 No. 15s, 2025
https://www.theaspd.com/ijes.php

Silver Doped Copper Oxide In Bio-Based Polyurethane Films-An Experimental Investigation For Electro-Mechanical Sensing

Basava T[1], Kishen Karumbaiah Bottangada Joyappa[2*], Raghu P A[3], Nithin Kundachira Subramani[4] and Sachhidananda Shivanna[5]

[1]*Visvesvaraya Technological University/ Professor, Mechanical Engineering Department, Sri Dharmasthala Manjunatheshwara Institute of Technology, Ujire, Karnataka State-574240, India.*
[*2]*Visvesvaraya Technological University/ Assistant Professor, Mechanical Engineering Department, Coorg Institute of Technology/ Ponnampet, Karnataka-571216, India.*
[3]*Selection Grade Lecturer, Mechanical Engineering Department, S.J.M. Polytechnic (Government Aided), Chitradurga, Karnataka- 577502, India.*
[4]*Excel Matnovous/ Director, Mysuru, Karnataka State-570018, India.*
[5]*Excel Matnovous/ Scientist B, Mysuru, Karnataka State-570018, India*

Abstract

Investigation aims at incorporation of metal-metal oxide nanoparticles by solution combustion method, into castor-oil based polyurethane following insitu polymerization technique and studied for structural, morphological, mechanical, thermal and electrical characterizations. Filler variations were maintained based on weight percentage in the study with film thickness within 1±0.1mm. Introduction of doping enhanced copper oxide conductive fillers into polyurethane resulted in increase of current conduction value by 10^4 times compared to pure films along with improved stretchability characteristics. Films with 4.0 weight percent filler recorded conductivity values upto 10^{-7} S/cm. Pure films show stretchability upto 59% before breakage, with less than 2% material degradation upto operating temperatures of 160°C.

Keywords: *Castor oil polyurethane film; Silver doped Copper oxide; electro mechanical characteristics, Thermal degradation.*

INTRODUCTION

Polyurethane (PU) is one of the most extensively utilized polymers due to its versatile characteristics, making it valuable across various industries, including manufacturing, automotive, sports, biomedical, and construction. PU is a linear block copolymer with alternating soft and hard segments that exhibit a phase-separated microstructure due to thermodynamic discordancy. Traditionally, petroleum-based raw materials such as polyols, catalysts, and isocyanates have been employed in the synthesis of PU, particularly Thermoplastic Polyurethane (TPU) [1]. However, recent advancements have shifted focus toward bio-based polyurethanes, which aim to replace petroleum-derived components with renewable materials. Although the transition to bio-based materials is promising, it presents challenges, including compromises in desired properties compared to petroleum-based PU. In recent years, bio-based polyols derived from natural resources such as vegetable oils (e.g., castor, soybean, sunflower, and rapeseed oils) have become well-established in the industry. Castor oil, in particular, is widely used due to its reactive hydroxyl (—OH) groups, which are beneficial for polyol synthesis. This oil is favoured for its availability, non-edibility, renewability, high purity, biodegradability, and cost-effectiveness. Despite these advantages, bio-based PUs often fall short of the performance levels provided by their petroleum-based counterparts. To enhance the properties of bio-based PU, researchers have explored various strategies, including the use of blends and composites. Fillers such as cellulose nanocrystals, clay, and wood flour have been incorporated into PU matrices, while blends with poly(lactic acid) and polyamide have been employed to improve mechanical and physical properties. Carbon nanotubes (CNTs) have been used as reinforcements in TPU matrices to enhance electrical and piezoresistive sensing characteristics [2]. Similarly, carbon black has

improved the viscoelastic and adhesive properties of PU, which are crucial for applications in additive manufacturing and flexible electronics. Graphene oxide and graphene platelets have also been added to TPU matrices to boost mechanical, thermal, sensing, piezoresistive, and shape memory properties. The effectiveness of these fillers largely depends on their dispersion and interaction with the PU matrix, as well as their shape, size, and morphology, which affect the electrically conductive network, especially for strain sensing applications. Several studies have explored various methods for synthesizing bio-based PU. Ivan et al. [3] synthesized PU from castor oil (CO) and toluene diisocyanate (TDI) without catalysts, maintaining a NCO to OH ratio of 1, under a nitrogen atmosphere at 110°C for 12 hours. Their findings indicated that adjusting the composition of starting materials and incorporating nanoparticles can enhance the thermal stability of PU materials. Yeganeh et al. [4] used CO dissolved in tetrahydrofuran with hexamethylene diisocyanate (HMDI) under a nitrogen atmosphere, stirring continuously until the theoretical NCO content was achieved, followed by vacuum drying at 50°C for up to 48 hours. Mileo et al. [5] employed compression molding with a CO and methylene diphenyl diisocyanate (MDI) prepolymer mixture in a 1.5:1 ratio, observing an exothermic reaction and a curing time of 48 hours. Ibrahim et al. [6] followed a transesterification process with MDI and glycerol, achieving a thermal glass transition temperature (Tg) of -15.8°C and thermal stability up to 259°C, with lithium salt addition enhancing conductivity. Ali et al. [7] used CO dehydrated in a vacuum oven, dissolved in TDI, and mixed with butanediol (BD) as a catalyst, maintaining a temperature of 65°C for 48 hours followed by a week-long post-curing at 80°C. This study demonstrated that multi-walled carbon nanotubes (MWCNTs) improved physicochemical properties, including thermal stability, reduced permeability, and mechanical strength. Further, Alaa et al. [8] synthesized viscous PU using the pre-polymer technique, with dehydrated poly(propylene glycol) reacted with diisocyanate and CO, using triethylenediamine and di(propylene glycol) as catalysts. Jun Zhang et al. [9] preheated CO with butanediol, mixed with MDI, and cured under 10 MPa pressure at 90°C for 1 hour, analyzing the materials using FTIR, DSC, TGA, DMA, XRD, tensile tests, and water absorption studies, achieving a tensile strength of 15.6 MPa and elongation at break of over 200%. Tan et al. [10] prepared PU films with CO and glycerol in varying ratios, stirred at 70°C in vacuum with equimolar MDI addition. Cuadri et al. [11] reacted CO with MDI at 60°C for 48 hours under nitrogen with continuous agitation, while Baheiraei et al. [12] synthesized prepolymer PU using chloroform and isophorone diisocyanate (IPDI), with DBTL as a catalyst, increasing temperature to 60°C and continuing the reaction until the free NCO content matched theoretical values. Macalino et al. [13] processed PU films with varying castor oil and HDMI ratios, achieving urethane linkages, hydrophilicity, thermal stability, and varying mechanical properties. Chethana et al. [14] obtained PU sheets by solution mixing CO in methyl ethyl ketone (MEK) with DBTL as a catalyst under oxygen-free heating, with hot air circulating mold curing for 10 hours. Khalifa et al. [15] prepared thermoplastic PU films with a constant ratio of CO, MDI, and BD, involving continuous stirring at 80°C with nitrogen blanketing and hot air curing for 16 hours. Santos et al. [16] prepared PU sheets from CO and MDI, maintaining an NCO to OH ratio of 1 with a curing time of 72 hours. Ganji et al. [17] synthesized PU with a 4:1:3 molar ratio of HMDI, PEG, and castor oil, stirred at 70°C with nitrogen and cured in a Teflon mold for 2 days. Luong et al. [18] prepared castor oil-segmented thermoplastic PU with DBTL in N-dimethylacetamide, using MDI as a catalyst, achieving elongation properties up to 1200%, excellent biocompatibility, recovery properties, and high transparency. Madhukar et al. [19] used an equal molar ratio of CO and TDI, dissolved in ethyl methyl ketone, with DBTL as a catalyst, continuous stirring, and curing at normal atmospheric conditions, followed by post-curing at 60°C. Mosiewicki et al. [20] utilized lithium hydroxide as a catalyst with triethanolamine and castor oil, maintaining stirring at 150°C for 2.5 hours. Chen et al. [21] prepared PU resins with an NCO to OH ratio of 1.5, using organosiloxane and water as surfactants and blowing agents, under normal atmospheric conditions with high-speed stirring. Shaik et al. [22] developed castor oil-based PU with TiO2 nanocomposites for anti-corrosive and antimicrobial coatings, using toluene-2,4-diisocyanate to modify castor oil-based polyesteramide. These coatings exhibited operational stability up to 200°C. Khalifa et al. [23] examined the physicochemical and piezoresistive strain sensing capabilities of a graphene-infused bio-based TPU thin film, prepared by solution casting,

with enhanced dispersion of graphene, resulting in improved physical properties and sensing performance, suitable for flexible electronics and structural health monitoring. The combination of bio-based PU with metal-metal oxides holds promise for applications in sensing and flexible electronics due to their excellent flexibility, strength, carrier mobility, and restorability. Recent research has highlighted the promising properties of alkali-doped metal oxides, which exhibit enhanced electrical conductivity, optical transparency, and structural stability. These attributes render them highly suitable for various optoelectronic and energy storage applications. Alkali metal incorporation into metal oxides significantly alters their electronic structures, affecting their band gap energy, carrier concentration, and optical characteristics. For example, doping with alkali metals can introduce excess electrons, thereby improving electrical conductivity. Tailoring the optical properties through selective doping enables the creation of transparent conductive oxides with high transmittance and low resistivity, which are ideal for applications such as solar cells and transparent electrodes [24-32]. Priscilla et al. [33] synthesized sodium-doped cupric oxide at the nanoscale using a solution combustion method and observed intriguing size-dependent chemical properties, including a high surface-to-volume ratio and unique electronic and optical characteristics. Their electrical analysis using AC impedance spectroscopy revealed a decrease in resistance with increased Na concentration, which they attributed to improved crystallinity and enhanced surface area. Siddiqui et al. [34] also studied Na-CuO nanostructures and found enhanced optical and electrical properties due to defect formations, such as copper and oxygen vacancies. Curda et al. [35] prepared AgCuO2 using a low-temperature route and reported promising properties for potential applications. Zhang et al. [36] developed conductive adhesive tapes by incorporating copper-silver nanoparticles and achieved a low volume resistivity of 2.0×10^{-6} Ωm. Vettumperumal et al. [37] analyzed Cs-ZnO thin films prepared via the sol-gel method, finding high mobility and improved crystalline quality, suggesting their suitability as transparent conductors. Additionally, Thangavel et al. [38] investigated the effects of cesium doping on ZnO thin films, noting significant changes in phonon energy and spectral properties, which could advance the development of optoelectronic devices. The integration of bio-based polyurethane further enhances the flexibility, strength, carrier mobility, and restorability of these materials, showcasing their potential across various applications. This study focuses on the development of bio-based PU/Ag-CuO nanocomposite thin films using the solution casting method, investigating their physicochemical characteristics, mechanical, thermal, and electrical properties, and electro active sensing capabilities. To the best of our knowledge, this represents the first report on such bio-based PU/Ag-CuO nanocomposite thin films.

2. EXPERIMENTATION

2.1 Materials

Analytical grade purified castor oil (CO) with 97% assay, methyl ethyl ketone (MEK), toluene-diisocynate (TDI) and dibutyl tin dilaurate (DBTL), cupric nitrate trihydrate, silver nitrate, glycine and sucrose. Procured chemicals were used as received from TCI chemicals Chennai, SD fine chemicals Mumbai, and Himedia laboratories Nasik, India.

2.2 Preparation of conductive polymer films

Silver doped copper metal oxide nanoparticles (Ag-CuO-NPs) are prepared by sol-gel method. The oxidizer was cupric nitrate, glycine and sucrose was fuel. Cupric nitrate, silver nitrate, sucrose and glycine is dissolved in doubly distilled water. The mixture is maintained at 60°C temperature with continuous stirring upto 5 hours until the solution mixture condensed into a gel form. The gel is subjected to further heating until auto ignition is attained and precipitation is observed. For completion of calcination process the combustion product is transferred to ceramic crucible and transferred into preheated muffle furnace for annealing at 800°C. The prepolymer was prepared from bio degradable castor oil with TDI and MEK as solvent and chain extender, more detailed preparation of the polymer has been discussed in our previous studies [31]. Prepolymer mixture was dispersed with calculated weight percent of Ag-CuO

nanoparticles and sonicated at 60°C in inert atmosphere. The films were transferred into glass moulds for 12 hrs of air drying and further curing of 8hrs at 70°C. Cured films were of 1±0.1 mm thickness and were cut into 10mm × 50mm strips for tensile and into 30 mm diameter circle for compressive testing.

2.3 Characterizations

Morphological structure was examined by obtaining scanning electron microscopy (SEM) images along with energy dispersive x-ray spectroscopy (EDX) reports. Composition and crystallinity of the films were investigated by spectrums obtained by x-ray diffraction (XRD) and fourier transform infrared (FTIR) Study. Particle distribution by Dynamic Light Scattering (DLS) technique, Tensile strength, compressive loading, electrical conductivity tests were conducted by universal testing machine (UTM) and keithley dc source meter. Thermal degradability tests were conducted by obtaining thermo gravimetric analysis (TGA) spectrums.

3. RESULTS AND DISCUSSIONS

3.1 XRD and DLS studies of Silver doped Copper Oxide Nanoparticles (Ag:CuO-NPs).

X-ray diffraction spectra of Ag:CuO-NPs is shown in Figure 1 . Obtained results are in well coordination with similar work by Iqbal et al. [39]. Diffraction peaks at 2θ values 32.5°, 35.5°, 38.1°, 48.7°, 53.5°, 58.3°, 61.6° and 68.1° are observed corresponding to monoclinic phase of CuO crystal planes. Peaks at 38.77°, 44.3°, 64.5° and 77.5° correspond to plane orientation (111), (220), (220) and (311) of Ag. All the diffraction peaks are in good agreement to monoclinic CuO (JCPDS no. 80-1917 and cubic Ag (JCPDS no. 04-0783 as reported [39]), indicating nanoparticles are composed of pure Ag:CuO. Particle distribution studies reveal average particles size of 76.94±1.28 nm which is in well agreement with previous studies.

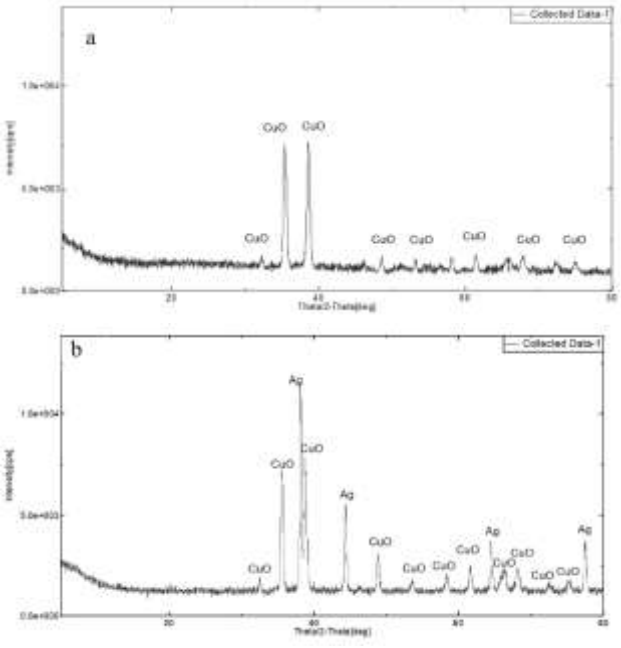

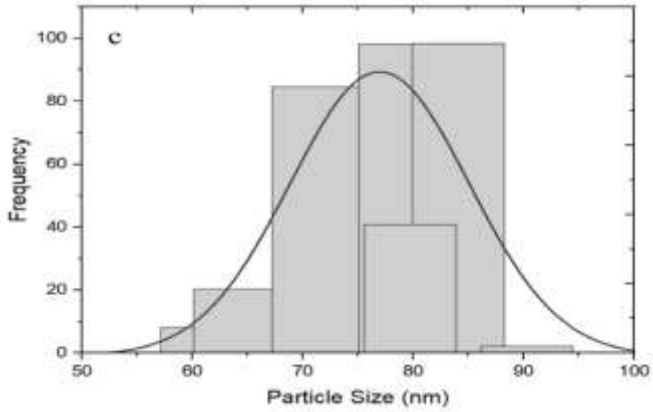

Figure 1 (a) Powder XRD spectra of Undoped Copper Oxide NPs (b) Powder XRD spectra of 5mol% Silver doped Copper Oxide NPs (Ag:CuO-NPs) (c) DLS particle distribution graph of the Ag:CuO fillers.

3.1 FTIR Characterization

The FTIR spectra for pure and filler dispersed PU nanocomposites for different filler weight percentages of 0.5, 1.0, 2.0 and 4.0% is as presented in Figure 2. The absence of the vibration band in the 1880cm^{-1} to 2800cm^{-1} range confirms the completion of urethane reaction and absence of free isocyanides group in the polymer structure [40,41]. Vibration bands at 1072cm^{-1}, 1550cm^{-1} to 1580cm^{-1} represent C-N stretching and N-H bending, peaks at 1600cm^{-1}and 1720cm^{-1} feature C-C and C-O stretching vibrations of urethane chains, bands between 2820cm^{-1} and 3040cm^{-1} show CH_2 symmetric and anti-symmetric stretching vibrations and 3380cm^{-1}features free O-H and N-H stretching [42-47]. With the addition and increase of Ag-CuO-NPs the peaks exhibit decreasing intensity. Increased stretching vibrations in 4000cm^{-1}to 3200cm^{-1} range is due to interaction of nanoparticles with urethane links [47].

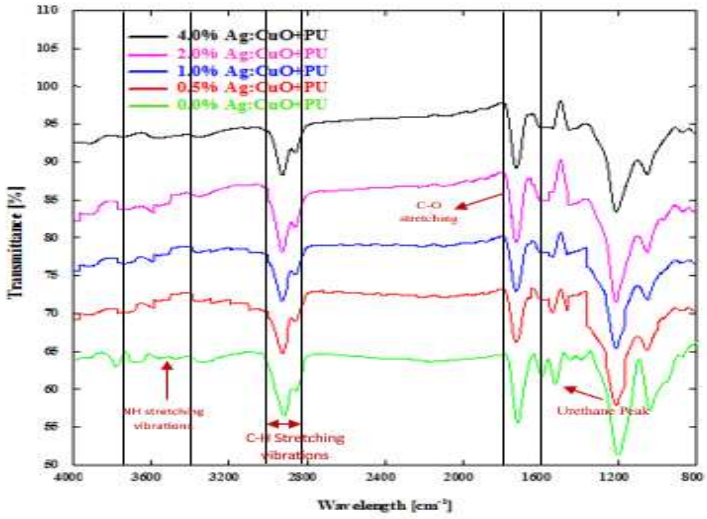

Group	Expected peaks (cm^{-1})	Observed absorption peaks (cm^{-1}) for Ag:CuO:PU composites
C=O	1714-1740	1720-1730
N-H stretching	3345-3400	3346-3330
Aromatic C-H stretching (symmetric and asymmetric stretching respectively)	2800-3100	2820-3040
C=C aromatic ring	1600 & 1430	1600
O ‖ -NH– C–NH (urethane peak)	1528	1536
C=O with hydrogen bonded	1650-1710	1697-1711
N-H stretching with hydrogen bonding	3260-3320	3380-3362

Figure2. Fourier transform infrared spectrum of pure and Ag-CuO NPs filled PU films.

3.2 XRD Characterization

XRD data of the undoped films, characteristic peaks are apparent at 2θ value of 20.3°. The corresponding reflection plane presents an interchain 'd' spacing measuring 4.369A°. Figure 3. The doped films, XRD spectrum unveils additional diffraction peaks at specific 2θ values, notably 32.5°, 41.1°, and 48.89°. These peaks suggest the embedded presence of CuO, further substantiated by the 'd' spacing of 2.32A°. Additional diffraction peaks at 2θ values of 35.0°, 38.33°, 58.33°, 61.66°, and 64.4° manifest within the doped film spectrum. These peaks are consistent with Ag-CuO, having 'd' spacing values ranging between 1.37A° to 1.44A°. Data provides compelling evidence for the successful incorporation of Ag-CuO nanoparticles within the PU matrix.

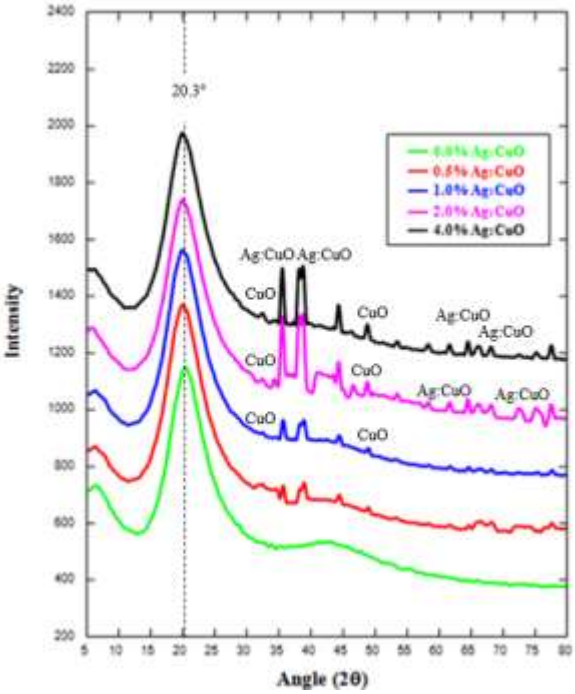

Figure 3. X-Ray Diffraction Spectrum of PU-Ag: CuO Nanocomposites, with Pristine, 0.5, 1.0, 2.0 and 4.0% NPs filler weight% dispersions.

3.3 Morphological and elemental characteristics

SEM images presented a specific morphological characteristic. Figure 4(a) unveils the microstructural facets of the unadulterated PU film. Evident from the image is a consistent and smooth surface, symbolizing the regular morphology generally associated with pure PU films. Such a uniform surface could potentially impact various material properties, including optical clarity and mechanical resilience. Figure 4(b), there is a marked shift in the microstructural appearance, this figure captures the presence of Ag-CuO nanoparticles within the polymer matrix. A observation is the manifestation of nano-sized agglomerations (average agglomeration size of 200nm). The literature suggests that such agglomeration phenomena can be attributed to a diminished radial growth rate in amorphous regions combined with inherently elevated surface energies [48,49].

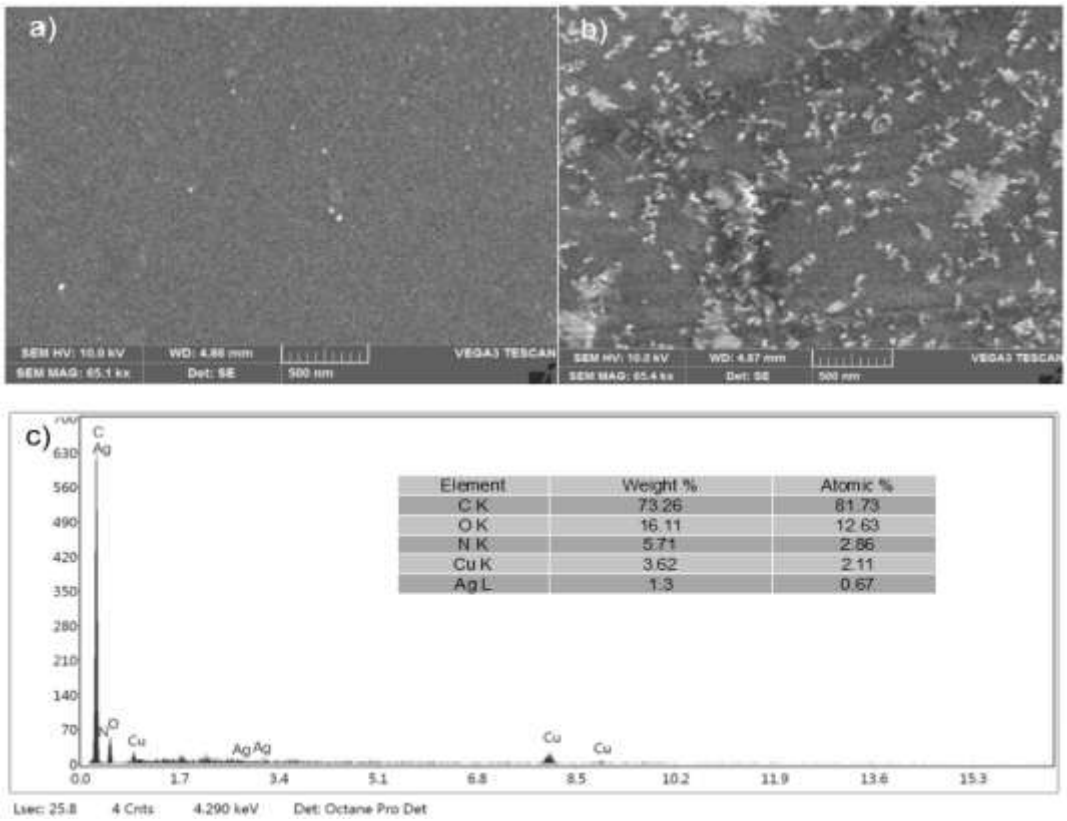

Figure 4. SEM images of (a) pristine and (b) Ag-CuO-Nps doped PU Film (c) EDX image of Ag-CuO-NPs PU film nano composite.

Elemental microanalysis of the formulated Polyurethane-Ag-CuO nanocomposites was executed, harnessing the capabilities of Energy dispersive Xray Spectroscopy (EDX) Figure 4c. Through the EDX assessment, several elemental constituents emerged, confirming the presence of Oxygen (O), Nitrogen (N), Carbon (C), Ag, and Cu within the nanocomposite structure. Intriguingly, Carbon, Oxygen, and Nitrogen stand out as the foundational elements constituting the PU matrix. The analytical data further illuminated distinct energy peaks, especially at the values of 0.52, 0.93, 1.04, 8.04, and 8.9keV. Elaborating on these findings, the X-ray energies at both 0.52 and 0.93keV were identified to be correlated with the emissions stemming from the K-shell of oxygen and the K-shell of copper, respectively. An energy peak at 3.01keV was associated with the L-shell emissions of Ag. The nanocomposite's elemental profile was further enriched by the emergence of supplementary energy peaks, notably at 0.52keV and 2.8keV. This enhancement in the energy spectrum can be attributed to the strategic doping of Ag within the CuO structure [50, 51-53].

3.4 Electro-Mechnical studies of nanocomposite films

Pure PU films were subjected to tensile testing show tensile strength of 0.152MPa with 59% elongation at breaking. On addition of nanoparticles films show decrement in tensile strength but increment in elongation stretchability. To study the change in conductivity of films with change in stretching distance, the films were attached with copper electrodes and connected to dc source meter, loaded to universal testing machine and subjected to tensile loading. Tensile deformation and current readings were recorded while the film was being stretched. Prepared conductive films were stretched to a maximum length of 10mm and the voltage potential was maintained constant at 50Volts. It can be observed that with the increment in filler weight percentage there is proportional increase in conductivity values at zero loading, as the stretching distance is increased there is drop in current conductivity ability of the films this is due to increase in inter-particle distance between fillers within the composite film. It is observed that there is

good coordination between tensile elongation and conductivity in films with filler weight percentages above 1.0wt%, below which the films exhibit constant values of current conduction for any value of stretch Figure 5(a) and 5(b).

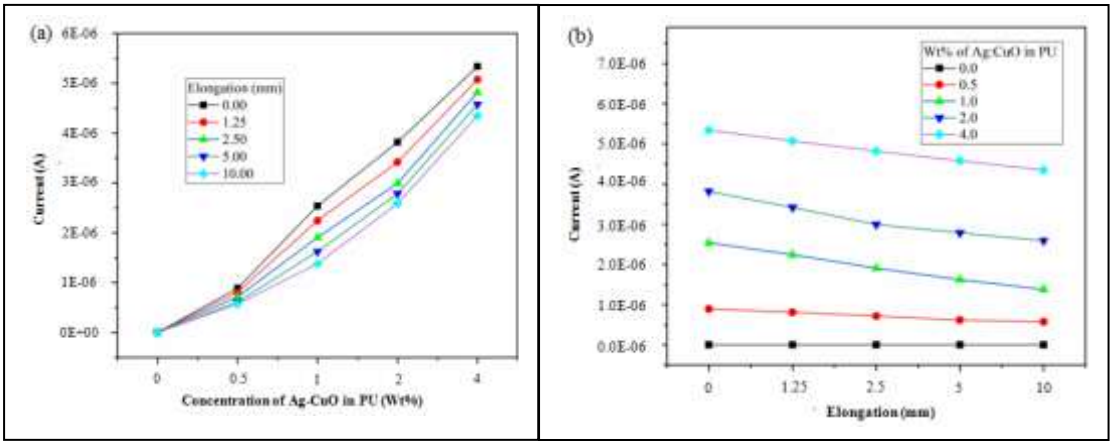

Figure 5. (a) Ag-CuO nanofiller weight concentration v/s current conductivity in films (b) tensile elongation v/s current conductivity of nanocomposite films.

To study the volume conductivity, films were subjected to compressive loading along with dc source meter attachment. The specimens were of 1mm thickness and cut into circular shapes with 30mm diameter sandwiched between copper electrodes. Examination of the films was achieved by loading the specimens in steps of five upto maximum load of 30N, after every new loading step, a settling duration of one minute was maintained and readings were recorded. Figure 6(a) shows linear increase in conductivity values with increment in loading. Films show no appreciable change in conductivity values upto a loading of 2.5N. With further increase in loading films tend to show linear increments of current conductivity. Considerable variations of current values above 15N loading were observed providing good range of workability. Figure 6(b) depicts the variation of conductivity with respect to filler concentration, doped films show linear increment in conductivity with increase in filler weight percentage. Maximum current conductivity value of $4.38E^{-5}$Amps or volume conductivity value of $1.317E^{-7}$S/cm is recorded at 50Volts of potential for nano composite films with filler percentage of 4.0wt% under a maximum load of 30N. All the tested films exhibited increase in conductivity values with load increment; this behaviour is due to tunnelling effect of nanofillers in the films.

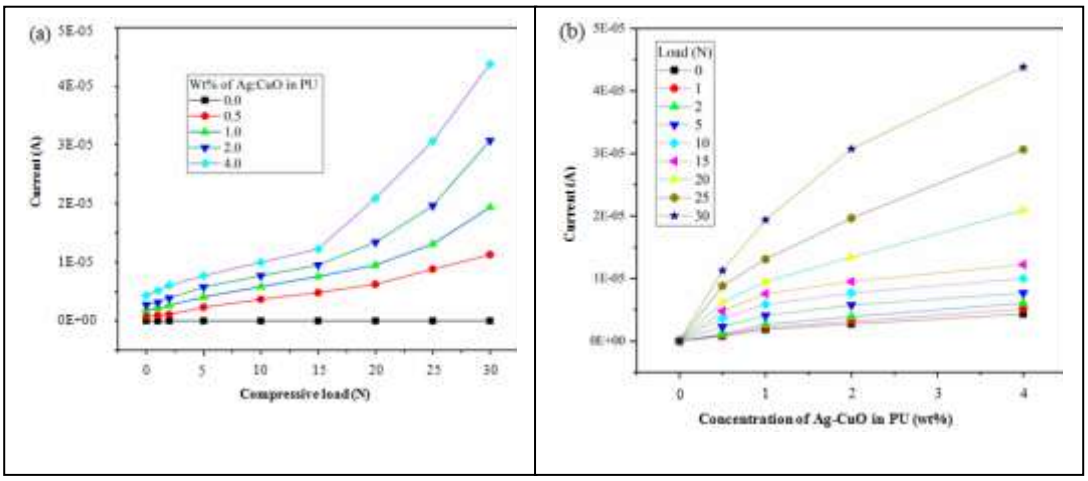

Figure 6. (a) Compressive load v/s current conductivity of films (b) Ag-CuO filler weight concentration versus conductivity of films under compression load.

3.5 Thermogravimetry Studies

Upon analysis of the thermal degradation properties of the films, Figure 7 displays significant weight loss of 50% recorded at 382°C because of degradation of the ester linkage connecting fatty acids to the glycerol backbone inherent in castor oil. The initial weight reduction of 10% occurs in films within temperature of 282°C. 80% of degradation in films was observed at temperature of 457°C, as a result of the breakdown of rigid segments within the PU structure [13,54]. Metallic oxide sediment remains accounted for 8.6% of sample weight at 900°C of testing temperature. Composite Films exhibit less than 2% of degradation loss up to operating temperature of 170°C.

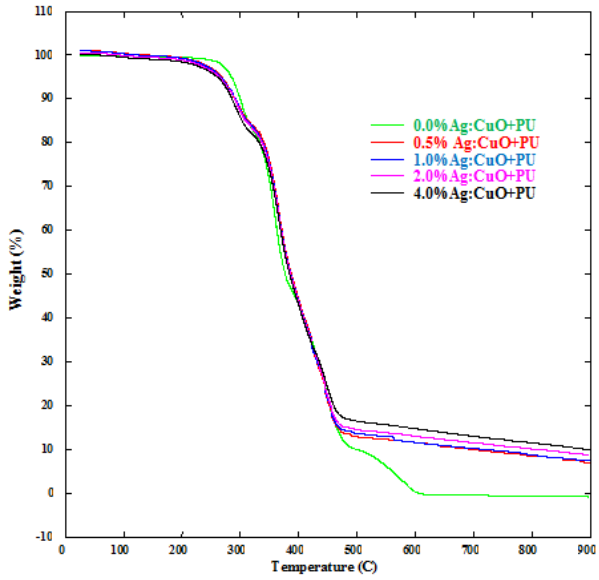

Figure 7. TGA Spectrum of Prestine PU and Ag-CuO-PU nanocomposite films showing average residual weight percentage of 8.6% in composite films.

4. CONCLUSIONS

Silver doped copper oxide nanoparticles were successfully prepared by sol gel method and dispersed into polyurethane prepolymer synthesized from bio-based polyol-castor oil. Films were subjected to studies by FTIR, XRD, DLS, SEM, EDAX, TGA and Electro-mechanical examinations. FTIR spectrums confirmed the formation of urethane links along with stretching vibration bands of Ag-CuO nano particles. XRD spectrum revealed the presence of Ag-CuO nanofillers in prepared films with diffraction peaks at 2θ values. EDAX analysis confirmed the presence of key urethane elements along with silver and copper in the films. Elongation versus conductivity tests reveal limitation of films to exhibit wider current conduction range so as to be used as sensing elements in stretching applications, whereas under compression loading films showed higher range of conduction above 15N loading. TGA analysis revealed less than two percent of total weight loss in films above 160°C of operational temperature.

REFERENCES:

[1] Aqdas Noreen, Khalid Mahmood Zia, Mohammad Zuber, Shazia Tabasum, Ameer Fawad Zahoor, Bio-based polyurethane: An efficient and environment friendly coating systems: A review, Progress in Organic Coatings, Volume 91, 2016, pp 25-32.

[2] Ke, K., Solouki Bonab, V., Yuan, D., & Manas-Zloczower, I. Piezoresistive thermoplastic polyurethane nanocomposites with carbon nanostructures. Carbon, 2018, 139, 52–58.

[3] Ristic, I.S., Bjelovic, Z.D., Hollo, B., Meszaros Szecsenyi, K., Budinski-Simendic, J., Lazic, N. and Kicanovic, M., Thermal stability of polyurethane materials based on castor oil as polyol component. Journal of thermal Analysis and Calorimetry, 2013, 111, pp.1083-1091.

[4] Yeganeh, H. and Hojati-Talemi, P., Preparation and properties of novel biodegradable polyurethane networks based on castor oil and poly (ethylene glycol). Polymer degradation and stability, 2007, 92(3), pp.480-489.

[5] Mileo, P.C., Mulinari, D.R., Baptista, C.A.R.P., Rocha, G.J.M. and Gonçalves, A.R., Mechanical behaviour of polyurethane from castor oil reinforced sugarcane straw cellulose composites. Procedia Engineering, 2011, 10, pp.2068-2073.
[6] Ibrahim, S., Ahmad, A. and Mohamed, N.S., 2015. Synthesis and characterization of castor oil-based polyurethane for potential application as host in polymer electrolytes. Bulletin of Materials Science, 2015, 38, pp.1155-1161.
[7] Ali, A., Yusoh, K. and Hasany, S.F., 2014. Synthesis and physicochemical behaviour of polyurethane-multiwalled carbon nanotubes nanocomposites based on renewable castor oil polyols. Journal of Nanomaterials, 2014, pp.165-165.
[8] Alaa, M.A., Yusoh, K. and Hasany, S.F., Pure polyurethane and castor oil based polyurethane: synthesis and characterization. Journal of Mechanical Engineering and Sciences, 2015, 8, pp.1507-1515.
[9] Zhang, J., Yao, M., Chen, J., Jiang, Z. and Ma, Y., 2019. Synthesis and properties of polyurethane elastomers based on renewable castor oil polyols. Journal of Applied Polymer Science, 2019, 136(14), p.47309.
[10] Tan, A.C.W., Polo-Cambronell, B.J., Provaggi, E., Ardila-Suárez, C., Ramirez-Caballero, G.E., Baldovino-Medrano, V.G. and Kalaskar, D.M., Design and development of low cost polyurethane biopolymer based on castor oil and glycerol for biomedical applications. Biopolymers, 2018, 109(2), p.e23078.
[11] Cuadri, A.A., García-Morales, M., Navarro, F.J. and Partal, P., 2013. Isocyanate-functionalized castor oil as a novel bitumen modifier. Chemical Engineering Science, 97, pp.320-327.
[12] Baheiraei, N., Gharibi, R., Yeganeh, H., Miragoli, M., Salvarani, N., Di Pasquale, E. and Condorelli, G., 2016. Electroactive polyurethane/siloxane derived from castor oil as a versatile cardiac patch, part I: Synthesis, characterization, and myoblast proliferation and differentiation. Journal of Biomedical Materials Research Part A, 2016, 104(3), pp.775-787.
[13] Macalino, A.D., Salen, V.A. and Reyes, L.Q., 2017, September. Castor oil based polyurethanes: synthesis and characterization. In IOP Conference Series: Materials Science and Engineering (Vol. 229, No. 1, p. 012016). IOP Publishing.
[14] Chethana, M., Madhukar, B.S., Siddaramaiah and Somashekar, R., Structure–property relationship of biobased polyurethanes obtained from mixture of naturally occurring vegetable oils. Advances in polymer technology, 2014, 33(1).
[15] Khalifa, M., Ekbote, G.S., Anandhan, S., Wuzella, G., Lammer, H. and Mahendran, A.R., Physicochemical characteristics of bio-based thermoplastic polyurethane/graphene nanocomposite for piezoresistive strain sensor. Journal of Applied Polymer Science, 2020, 137(44), p.49364.
[16] Dos Santos, D.J., Tavares, L.B. and Batalha, G.F., 2012. Mechanical and physical properties investigation of polyurethane material obtained from renewable natural source. Journal of Achievements in Materials and Manufacturing Engineering, 2012, 54(2), pp.211-217.
[17] Ganji, Y., Kasra, M., Kordestani, S.S. and Hariri, M.B., Synthesis and characterization of gold nanotube/nanowire–polyurethane composite based on castor oil and polyethylene glycol. Materials Science and Engineering: C, 2014, 42, pp.341-349.
[18] Dang, L.N., Le Hoang, S., Malin, M., Weisser, J., Walter, T., Schnabelrauch, M. and Seppälä, J., 2016. Synthesis and characterization of castor oil-segmented thermoplastic polyurethane with controlled mechanical properties. European Polymer Journal, 2016, 81, pp.129-137.
[19] Madhukar, B.S., Bhadre Gowda, D.G., Annadurai, V., Somashekar, R. and Siddaramaiah, 2016. Phase behaviors of pu/spi green composites using saxs profiles. Advances in Polymer Technology, 35(1).
[20] Mosiewicki, M.A., Dell'Arciprete, G.A., Aranguren, M.I. and Marcovich, N.E., Polyurethane foams obtained from castor oil-based polyol and filled with wood flour. Journal of composite materials, 2009, 43(25), pp.3057-3072.
[21] Chen, Y.C. and Tai, W., Castor oil-based polyurethane resin for low-density composites with bamboo charcoal. Polymers, 2018, 10(10), p.1100.
[22] Shaik, M.R., Alam, M. and Alandis, N.M., 2015. Development of castor oil based poly (urethane-esteramide)/TiO2 nanocomposites as anticorrosive and antimicrobial coatings. Journal of nanomaterials, 2015, 16(1), pp.176-176.
[23] Khalifa, M., Ekbote, G.S., Anandhan, S., Wuzella, G., Lammer, H. and Mahendran, A.R., Physicochemical characteristics of bio-based thermoplastic polyurethane/graphene nanocomposite for piezoresistive strain sensor. Journal of Applied Polymer Science, 2020, 137(44), p.49364.
[24] Macleod, Claire & Harvey, Adam & Lee, Adam & Wilson, Karen. Evaluation of the activity and stability of alkali-doped metal oxide catalysts for application to an intensified method of biodiesel production. 2008, Chemical Engineering Journal. 135.

[25] Nolan, Michael ; Watson, Graeme W et al. The electronic structure of alkali doped alkaline earth metal oxides: Li doping of MgO studied with DFT-GGA and GGA + U, Surface Science, 2005, Volume 586.
[26] Rane, V. & Chaudhari, Shivani & Choudhary, Vasant., Influence of alkali metal doping on surface properties and catalytic activity/selectivity of CaO catalysts in oxidative coupling of methane. Journal of Natural Gas Chemistry - J Nat Gas Chem. 17. 2008.
[27] Sunaina Wajid et al. Demonstrating the Potential of Alkali Metal-Doped Cyclic C6O6Li6 Organometallics as Electrides and High-Performance NLO Materials, ACS Omega 2021, 6, 44, 29852–29861
[28] Cuadra, J.G.; Porcar, S.; Fraga, D.; Stoyanova-Lyubenova, T.; Carda, J.B, Enhanced Electrical Properties of Alkali-Doped ZnO Thin Films with Chemical Process. Solar 2021.
[29] B. J. Kishen Karumbaiah, et al., "Nanotechnology-enabled polymer-based flexible electronics and their potential applications", in Polymer-Based Advanced Functional Composites for Optoelectronic and Energy Applications, ed by K S Nithin, H Siddaramaiah and Joong Hee Lee, Elsevier Publications, 2021, pp.321-340.
[30] K. S. Nithin, et al., "Polymer-Based Advanced Functional Composites for Optoelectronic and Energy Applications", in Polymer-Based Advanced Functional Composites for Optoelectronic and Energy Applications, ed by K S Nithin, H Siddaramaiah and Joong Hee Lee, Elsevier Publications, 2021, pp. 291-320.
[31] B. J. Kishen Karumbaiah, T. Basava, K. S. Nithin and S. Sachhidananda. "Experimental Study and Characterization of Conductive Metal Oxide Nanoparticle incorporated polyurethane films for sensing Application", European Chemical Bulletin, Special 2023, Issue 9, pp. 1706-1713.
[32] B. J. Kishen Karumbaiah et al 2024 J. Phys.: Conf. Ser. 2748 012005
[33] Priscilla, S.J., Sivaji, K. and Vimaladevi, L., May. Synthesis and characterization of Na doped cupric oxide (CuO) nanoparticles. In AIP conference proceedings, 2017, Vol. 1832, No. 1). AIP Publishing.
[34] Siddiqui, H., Parra, M.R., Qureshi, M.S., Malik, M.M. and Haque, F.Z., Studies of structural, optical, and electrical properties associated with defects in sodium-doped copper oxide (CuO/Na) nanostructures. Journal of materials science, 2018, 53(12), pp.8826-8843.
[35] Curda, J., Klein, W. and Jansen, M., $AgCuO_2$ synthesis, crystal structure, and structural relationships with CuO and AgIAgIIIO2. Journal of Solid State Chemistry, 2001, 162(2), pp.220-224.
[36] Zhang, J., Liang, M., Hu, Q., Ma, F., Li, Z., Wang, Y., Wang, L. and Zhang, S., Cu@ Ag nanoparticles doped micron-sized Ag plates for conductive adhesive with enhanced conductivity. International Journal of Adhesion and Adhesives, 2020, 102, p.102657.
[37] Vettumperumal, R., Kalyanaraman, S. and Thangavel, R., Sol–Gel Processed Cs-Doped ZnO Thin Films for Transparent Conductor Applications. Advanced Science, Engineering and Medicine, 2016, 8(9), pp.705-710.
[38] Thangavel, R., Singh Moirangthem, R., Lee, W.S., Chang, Y.C., Wei, P.K. and Kumar, J., 2010. Cesium doped and undoped ZnO nanocrystalline thin films: a comparative study of structural and micro-Raman investigation of optical phonons. Journal of Raman Spectroscopy, 41(12), pp.1594-1600.
[39] Shahid Iqbal et al., Controlled synthesis of Ag-doped CuO nanoparticles as a core with poly(acrylic acid) microgel shell for efficient removal of methylene blue under visible light", Journal of Materials Science: Materials in Electronics. 2020.
[40] A. C. W. Tan, et al., "Design and development of low cost polyurethane biopolymer based on castor oil and glycerol for biomedical applications", Biopolymers. 2018, vol. 109 issue 2.
[41] Jun Zhang, Ming Yao, Jianjun Chen, Zhiguo Jiang and Yuhong Ma, "Synthesis and properties of polyurethane elastomers based on renewable castor oil polyols", *Journal of Applied Polymer Science*, 2018, vol 136, issue 14.
[42] Salmiah Ibrahim, Azizan Ahmad and Nor Sabirin Mohamed, "Characterization of Novel Castor Oil-Based Polyurethane Polymer Electrolytes," *Polymers*, 2015, pp. 747-759.
[43] Kishore K. Jena, D.K. Chattopadhyay and K.V.S.N. Raju, "Synthesis and characterization of hyper branched polyurethane-urea coatings," European. Polymer Journal, 2007, vol. 43, pp. 1825–1837.
[44] Suman Thakur and Niranjan Karak, "Castor oil-based hyperbranched polyurethanes as advanced surface coating materials". Progress in Organic Coatings, 2013, vol. 76, issue 1, pp. 157–164.
[45] AD Macalino, VA Salen and LQ Reyes, "Castor Oil Based Polyurethanes: Synthesis and Characterization," in IOP Conference Series in Materials Science and Engineering, 2016, 229(1).
[46] Khairiah Binti, et al., "FTIR Spectroscopy Analysis of The Pre-polymerization Of Palm-Based Polyurethane" Solid State Science and Technology, 2010, Vol. 18, No 2, pp. 1-8.
[47] R. Nirmala, Kyung Soo Jeon, Baek Ho Lim, R. Navamathavan and Hak Yong Kim, "Preparation and characterization of copper oxide particles incorporated polyurethane composite nanofibers by electro-spinning" Ceramics International, 2013, vol. 39, issue8, pp. 9651–9658.

[48] Khan, S.A., Rahman, A., Khan, W. and Haider, S.M., Characterization and application of nano-composite zinc oxide/poly vinyl alcohol thin-film in solar cell performance enhancement. Journal of Mechanical Science and Technology, 2023, pp.1-11.
[49] Aslam, M., Kalyar, M.A. and Raza, Z.A., 2021. Fabrication of nano-CuO-loaded PVA composite films with enhanced optomechanical properties. Polymer Bulletin, 2021, 78, pp.1551-1571.
[50] Kiran, R., Prakash, K.R., Chandra, P., Kumar, V.R., Asha, P.B. and Rao, C.P., 2021. Experimental study on polymer nanocomposites based strain sensors for structural health monitoring. Journal of Minerals and Materials Characterization and Engineering, 2021, 9(5), pp.512-527.
[51] Yallappa, S., Manjanna, J., Dhananjaya, B.L., Vishwanatha, U., Ravishankar, B., Gururaj, H., Niranjana, P. and Hungund, B.S., 2016. Phytochemically functionalized Cu and Ag nanoparticles embedded in MWCNTs for enhanced antimicrobial and anticancer properties. Nano-micro letters, 2016, 8, pp.120-130.
[52] Amargeetha, A. and Velavan, S., X-ray diffraction (XRD) and energy dispersive spectroscopy (EDS) analysis of silver nanoparticles synthesized from Erythrina indica flowers. Nanosci. Technol. 2018, 5, pp.1-5.
[53] Mohamad, N.A.N., Arham, N.A., Junaidah, J., Hadi, A. and Idris, S.A., May. Green synthesis of Ag, Cu and AgCu nanoparticles using palm leaves extract as the reducing and stabilizing agents. In IOP Conference Series: Materials Science and Engineering 2018, Vol. 358, p. 012063.
[54] Chiang et al. Dopant effects on conductivity in copper oxide photoelectrochemical cells. Applied Energy. , 2015, 164. 10.1016/j.apenergy.2015.01.116.